

DEM analyses of the whole failure process of shallow foundation in plate load test on dense sand

L Li^{1,2,3,5}, M J Jiang^{1,2,3}, T Li^{1,2,3} and S L Chen⁴

¹ State Key Laboratory for Disaster Reduction in Civil Engineering, Tongji University, Shanghai 200092, China

² Key Laboratory of Geotechnical and Underground Engineering of Ministry of Education, Tongji University, Shanghai 200092, China

³ Department of Geotechnical Engineering, Tongji University, Shanghai 200092, China

⁴ Transportation and Municipal Engineering Institute, Hydrochina Huadong Engineering Corporation, Hangzhou 310014, China

E-mail: lilei_tongji@126.com

Abstract. Shallow foundations are widely used in civil engineering practice, but the instability mechanism is still unclear yet. Previously, the Finite Element Method (FEM) was commonly used to analyze the failure process of shallow foundations, but it meets difficulty in properly simulating the whole failure process of shallow foundation on the strain-softening material. Hence, the Discrete Element Method (DEM) is employed in this paper to study the instability mechanism of the shallow foundation via numerical plate load test with focus on the microscopic features evolution during vertical loading. In the simulation, an amplified gravity was applied to a dense granular ground to reproduce a gravity stress state at a large scale. Then, a plate was put on the granular ground to simulate the plate load test. Deformation pattern, particle velocity and distribution of void ratio in the ground were examined to illustrate the microscopic features in the whole failure process of the granular ground. The results show that: 1) There are a marked peak value and a settlement softening branch in the stress-settlement relationship. 2) The grids close to the edge of the plate are peculiarly extended and twisted. 3) Four particle motion patterns were observed in the velocity fields and the percentage of each motion pattern changes during loading. 4) The void ratio field varies during loading, and the distinguishing interface tends to be similar to Terzaghi's shear failure surface.

1. Introduction

The shallow foundation, one of the two classic foundation categories - shallow foundation and deep foundation, has been widely used in geotechnical engineering practice. In the traditional research, some macroscopic phenomena such as the relationship between stress and settlement were studied by the laboratory and in-situ plate load tests. However, the microscopic features in the ground, such as particle velocity and distributions of void ratio, cannot be observed. In recent decades, by simulating plate load test using the Finite Element Method (FEM) and finite-difference method [1-5], some microscopic features in the ground were observed. Nevertheless, there are some shortcomings using the continuum numerical method ascribe to some limitations including constitutive model and the

⁵ To whom any correspondence should be addressed.



assumption of small deformation. For example, when the bearing capacity neither increases gradually nor keeps stable with the increase in settlement, the features cannot continually reflect the ground's status correctly.

An alternative tool, the Discrete Element Method (DEM) developed by Cundall and Strack [6], has been used more and more widely in geotechnical engineering to obtain mechanical behaviors of soil samples [7-11], and to investigate the responses of soils under different boundary conditions [12-16]. More importantly, this numerical analysis technique can provide not only observations on the macroscopic mechanical response of a particle assemblage but also insights into the microscopic mechanical information.

The main aim of this paper is to study on the plane-strain instability mechanism in granular material with focus on the microscopic features in the whole failure process of the shallow foundation on dense sand. For the purpose, the plate load test was carried out on the granular ground with K_0 boundary. Relationship between stress and settlement, deformation pattern, velocity field and void ratio field are analyzed in the failure process.

2. Sand ground specimen

The material used in the ground is composed of 15 types of discs. The maximum and minimum diameter of the granular particles is 0.5 mm and 2.0 mm, respectively. The mean particle diameter is $d_{50}=1.3$ mm and the uniformity coefficient is $C_u=d_{60}/d_{10}=2.4$. Due to the geometric symmetry of the boundary-value problem, only a half of the ground and plate was generated using the DEM in the simulation. The target ground consists of 160,000 particles with planar void ratio of about 0.18, and has a width and depth of $W=0.48$ m and $D=0.3$ m, respectively. The multi-layer under-compaction method (UCM) proposed by Jiang et al.[17] was used to generate the ground. In order to improve the homogeneity, the wall-particle frictional coefficient is set to be zero, and inter-particle frictional coefficient (μ) is also set to be zero in the ground generation in order to produce a dense assembly of particles. After the ground was generated, the inter-particle frictional coefficient is chosen to be 1.0, and then the granular ground was consolidated under an amplified gravity field of 10 g. After the ground was consolidated, a loading plate with a width of $B/2=0.06$ m is formed at the central line as shown in Figure. 1. The loading plate represented by a rigid wall is then pushed downward at a velocity of 5.0×10^{-3} m/s. The frictional coefficient between the loading plate and particle is set to be 1.0 in the process of loading.

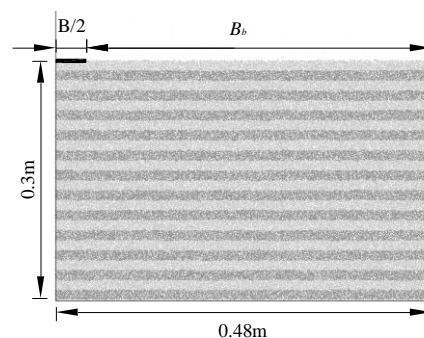


Figure 1. Boundary conditions of the ground in the DEM analyses.

3. Macroscopic strength features of the ground material

The macro mechanical behavior of the ground specimen was studied by conducting DEM simulation of biaxial tests. The DEM specimen for the biaxial tests consisting of 6,000 particles was compressed at a strain rate of 5%/min under the confining stresses of 50 kPa, 100 kPa, 200 kPa and 400 kPa, respectively. These biaxial tests indicate that the peak and residual internal friction angle of the material is 31° and 12° , respectively.

4. Simulation results

4.1. Relationship between stress and settlement

Figure 2 presents that the vertical stress on the rough foundation exists a peak value which decreases sharply to a residual value with the increase in the foundation settlement. The residual value decreases slightly with the increase in the foundation settlement. In order to analyze the instability mechanism of the ground in the whole process of the plate load test, the relationship curve between stress and settlement can be divided into four sections. As shown in Figure 2, the first section from the point of origin to point A can be named as compression stage, the second section from point A to point C can be named as shear stage, the third section from point C to point D can be named as softening stage, and the last section from point D to the end can be named as residual stage. At the points (A, B, C and D) on the curve, deformation pattern, particle velocity and distributions of void ratio in the ground were observed to investigate the evolution of the granular ground.

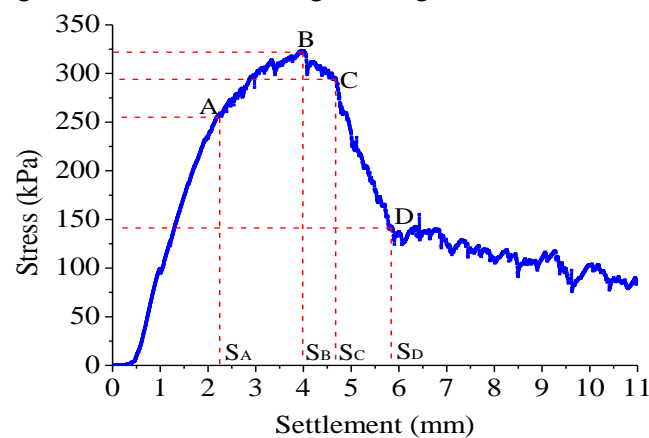


Figure 2. Relationship between stress and settlement in the plate load test.

4.2. Deformation fields

Figure 3 presents the painted grids observed in the plate load test at different settlements. The painted grid method proposed by Jiang et al. [18] was adopted to show the deformation pattern of the granular ground.

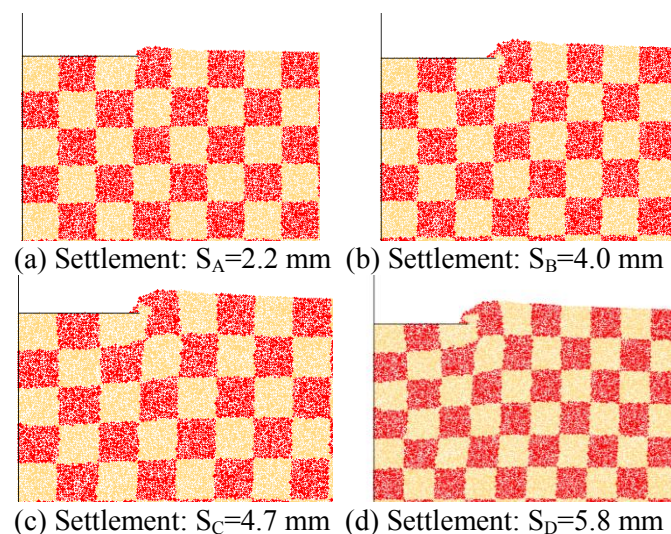


Figure 3. Deformation fields in granular ground

At the end of the compression stage, see Figure 3(a), the plate has slight influence on the painted grids which basically keeps the original shape. When the vertical stress comes to the peak value of the ultimate bearing capacity as shown in Figure 3(b), the top-right grid under the plate is pushed sideward and upward while the top-left grids under the plate are pushed down. In contrast, the top grid to the right of the plate is “dragged” downward and sideward. At the end of the shear stage and the end of the softening stage, see Figure 3(c) and (d), the top-right grid under the plate is pushed downward, sideward and upward, and the grid to the right of the top-right grid is squeezed sideward, downward and upward, hence these grids are peculiarly extended and twisted. The deformation of these grids is very difficult to be described properly with the “elements” used in conventional finite element analysis.

4.3. Velocity fields

Figure 4 presents the velocity vectors of all particles which were colored based on their velocity magnitudes. These velocity vectors were divided into seven intervals with their velocities from zero to the maximum velocity v_{max} and presented by vectors with seven colors.

Figure 4 provides velocity fields observed at different settlements: $S_A=2.2$ mm (a), $S_B=4.0$ mm (b), $S_C=4.7$ mm (c) and $S_D=5.8$ mm (d). Figure 4 shows that velocity field is different at different settlements. In Figure 4(a), i.e. in the compression stage, most of the particles under the plate move downward while some particles beneath the edge of the plate downward and sideward. The particles to the right of the plate and under the plate are affected by the plate movement. In the granular ground, four particle motion patterns are observed: downward, downward and sideward, sideward, sideward and upward. Figure 4(b) shows that when the vertical stress comes to the peak value, the number of particles to the right of the plate moving sideward and upward increases significantly compared with that of the compression stage while the number of particles under the plate moving downward decreases obviously. In Figure 4(c) and (d), the aforementioned four motion patterns of particles still exist in the granular ground, but the number of the particles moving downward decreases gradually. In addition, the shear interface tends to be similar to Terzaghi’s shear failure surface [6].

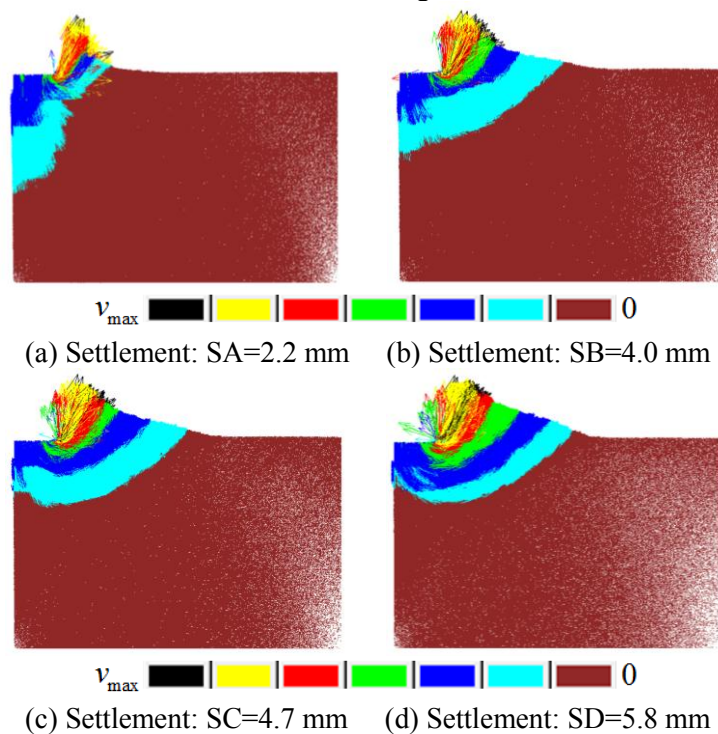


Figure 4. Distributions of velocity vectors in the DEM analyses

4.4. Void ratio fields

The void ratio is a classical variable in soil mechanics, but it is very difficult to describe the variable properly by the FEM when dilation appears in the soil. In contrast, the void ratio field in the granular ground can be easily measured by measurement circle in the DEM analysis.

Figure 5 provides the distribution of the void ratios observed at settlements of $S_A=2.2$ mm (a), $S_B=4.0$ mm (b), $S_C=4.7$ mm (c), and $S_D=5.8$ mm (d). Figure 5(a) shows that the expansion area (the void ratio increases within the area) is significantly located at the region close to the edge of the plate. When the stress comes to the peak value in Figure 5(b), the expansion occurs in a larger area, and a through-interface is formed preliminarily. In Figure 5(c) and (d), it is obvious that the expansion only occurs in a specific area at which the void ratio increases during loading, and the distinguishing interface tends to be similar to Terzaghi's shear failure surface [6].

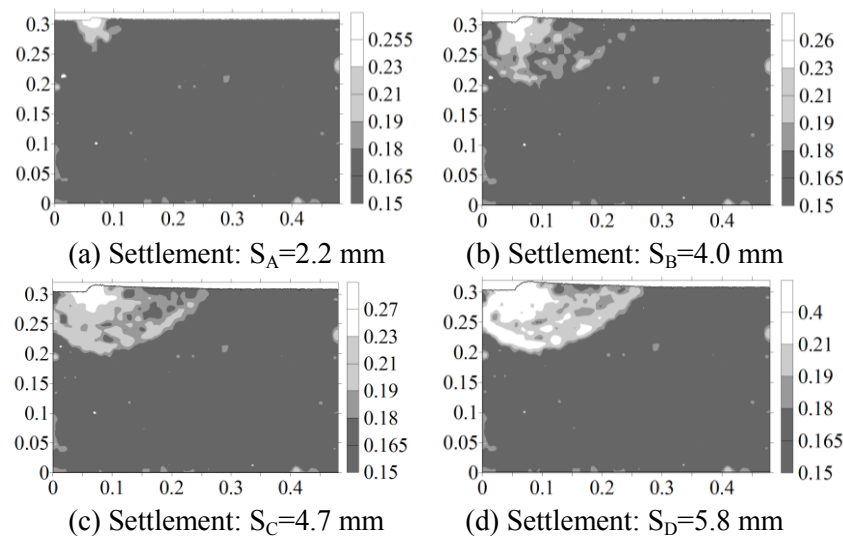


Figure 5. Distributions of void ratio in the granular ground

5. conclusions

The discrete element method numerical technique was used to investigate the failure process of the shallow foundation on dense sand ground by simulating plate load test. Deformation pattern, velocity field and void ratio field are analyzed to study on the plane-strain instability mechanism with focus on the microscopic features in the granular ground. The main conclusions are as follows:

- 1) The relationship curve between stress and settlement can be divided into four stages: compression, shear, softening and residual stages.
- 2) The grids are pushed towards many directions so that some grids close to the edge of the plate are peculiarly extended and twisted.
- 3) In the velocity fields, four particle motion patterns are observed: downward, downward and sideward, sideward, sideward and upward. The percentage of each motion patterns changes during loading. In addition, the shear interface tends to be similar to Terzaghi's shear failure surface.
- 4) The void ratio field varies during loading as well. The distinguishing interface tends to be similar to Terzaghi's shear failure surface.

Acknowledgements

The research was funded by the National Basic Research Program of China (973 Program) with grant Nos. 2014CB046901 and 2011CB013504, the State Key Laboratory of Disaster Reduction in Civil Engineering with Grant No. SLDRCE14-A-04, and the China National Funds for Distinguished Young Scientists with grant No. 51025932. All of these supports are greatly appreciated.

References

- [1] Yin J H, Wang Y J, and Selvadurai A P S 2001 Influence of nonassociativity on the bearing

- capacity of a strip footing *J. Geotech. Geoenviron. Eng.* **127** 985-989
- [2] Erickson H L, and Drescher A 2002 Bearing capacity of circular footings *J. Geotech. Geoenviron. Eng.* **128** 38-43
 - [3] Hjiat M, Lyamin A V, and Sloan S W 2005 Numerical limit analysis solutions for the bearing capacity factor N_γ *Int. J. Solids Struct.* **42** 1681-1704
 - [4] Lyamin A V, Salgado R, Sloan S W, and Prezzi M 2007 Two-and three-dimensional bearing capacity of footings in sand *Géotechnique* **57** 647-662
 - [5] Loukidis D, and Salgado R 2009 Bearing capacity of strip and circular footings in sand using finite elements *Comput. Geotech.* **36** 871-879
 - [6] Cundall P A, Strack O D L 1979 A discrete numerical model for granular assemblies *Géotechnique* **29** 47-65
 - [7] Jiang M J, Zhang F G, Hu H J, Cui Y J, and Peng J B 2014 Structural characterization of natural loess and remolded loess under triaxial tests *Eng. Geol.* **181** 249-260.
 - [8] Jiang M J, Chen H, Tapias M, Attoyo M, and Fang L 2014 Study of mechanical behaviour and strain localization of methane hydrate bearing sediments with different saturations by a new DEM model *Comput. Geotech.* **57** 122-138
 - [9] Jiang M J, Yan H B, Zhu H H, and Utili S 2011 Modeling shear behaviour and strain localization in cemented sands by two-dimensional distinct element method analyses *Comput. Geotech.* **38** 14-29
 - [10] Jiang M J, Li T, Hu H J, and Thornton C 2014 DEM analyses of one-dimensional compression and collapse behaviour of unsaturated structural loess *Comput. Geotech.* **60** 47-60
 - [11] Jiang M J, Liu J D, Sun Y G, and Yin Z Y 2013 Investigation into macroscopic and microscopic behaviors of bonded sands using distinct element method *Soils Found.* **53** 804-819
 - [12] Jiang M J, Dai Y S, Cui L, Shen Z F, and Wang X X 2014 Investigating mechanism of inclined CPT in granular ground using DEM *Granul. Matter* **16** 785-796
 - [13] Jiang M J, He J, Wang J F, Liu F, and Zhang W C 2014 Distinct simulation of earth pressure against a rigid retaining wall considering inter-particle rolling resistance in sandy backfill *Granul. Matter* **16** 797-814
 - [14] Jiang M J, and Yin Z Y 2012 Analysis of stress redistribution in soil and earth pressure on tunnel lining using the discrete element method *Tunn. Undergr. Sp. Tech.* **32** 251-259
 - [15] Jiang M J, Shen Z F, and Zhu F Y 2013 Numerical analyses of braced excavation in granular grounds: continuum and discrete element approaches *Granul. Matter* **15** 195-208
 - [16] Jiang M J, and Murakami A 2012 Distinct element method analyses of idealized bonded-granulate cut slope *Granul. Matter* **14** 393-410
 - [17] Jiang M J, Konrad J M, and Leroueil S 2003 An efficient technique for generating homogeneous specimens for DEM studies *Comput. Geotech.* **30** 579-597
 - [18] Jiang M J, Yu H S, and Harris D 2006 Discrete element modelling of deep penetration in granular soils *Int. J. Numer. Anal. Met.* **30** 335-361